

EVIDENCE FOR A 20 PARSEC DISK AT THE NUCLEUS OF CENTAURUS A¹

ETHAN J. SCHREIER, ALESSANDRO MARCONI,^{2,3} DAVID J. AXON,^{4,5} NICOLA CAON, AND DUCCIO MACCHETTO⁴

Space Telescope Science Institute, 3700 San Martin Drive, Baltimore, MD 21218

ALESSANDRO CAPETTI

Osservatorio Astronomico di Torino, Strada Osservatorio 20, I-10025 Pino, Torinese, Italy

JAMES H. HOUGH AND STUART YOUNG

Division of Physics and Astronomy, Department of Physical Sciences, University of Hertfordshire, College Lane, Hatfield, Herts AL10 9AB, England, UK

AND

CHRIS PACKHAM

Isaac Newton Group, Sea Level Office, Apartado de Correos, 321, 38780 Santa Cruz de La Palma, Islas Canarias, Spain

Received 1997 December 29; accepted 1998 April 3; published 1998 May 14

ABSTRACT

We report *Hubble Space Telescope* NICMOS observations of the central region of NGC 5128 at 2.2 μm and in Pa α . The continuum images show extended emission typical of an elliptical galaxy and a strong unresolved central source we identify as the nucleus of the galaxy. Its position is consistent with ground-based IR and radio data, and with the peak of reddening found with the first wide field planetary camera. In Pa α , we detect a prominent elongated structure, centered on the nucleus, extended by $\approx 2''$ at a position angle of $\approx 33^\circ$, and with a major to minor axis ratio of ~ 2 . We interpret this as an inclined, ~ 40 pc diameter, thin nuclear disk of ionized gas rather than a jet-gas cloud interaction. We do see several weaker Pa α features, some of which may be circumnuclear gas clouds shocked by the X-ray/radio jet. The disk is one of the smallest ever observed at the nucleus of an active galactic nucleus (AGN). It is not perpendicular to the jet but is consistent with being oriented along the major axis of the bulge. If it represents the warped outer portion of an accretion disk around a black hole, we conclude that even on the scale of a few parsecs, the disk is dominated by the galaxy gravitational potential and is not directly related to the symmetry axis of the AGN.

Subject headings: galaxies: active — galaxies: individual (NGC 5128, Centaurus A) — galaxies: Seyfert

1. INTRODUCTION

NGC 5128 (Centaurus A), the nearby giant elliptical galaxy, hosts the closest powerful active galactic nucleus. This double-lobed radio source contains a strong jet discovered in X-rays (Schreier et al. 1979; Feigelson et al. 1981) and well-studied in radio with the VLA (Schreier, Burns, & Feigelson 1981; Burns, Feigelson, & Schreier 1983; Clarke, Burns, & Feigelson 1986) and with the VLBI (see Jones et al. 1996). The proximity of NGC 5128 makes it one of the best candidates for studying the inner region around a massive black hole, assumed by the standard model to be at the core of all AGNs (see, e.g., Blandford 1991; Antonucci 1993). However, the large warped dust lane, approximately $1'$ wide with associated gas, young stars, and H II regions, dominates the morphology and polarization properties at visible wavelengths, effectively obscuring the nucleus and inner half kiloparsec of the galaxy and the jet.

Ground-based IR observations have provided evidence for a strong, heavily polarized source at the nucleus (see Bailey et al. 1986; Packham et al. 1996). Previous *Hubble Space Telescope* (*HST*) first wide field planetary camera (WFPC 1) imaging polarimetry of the inner region of NGC 5128 (Schreier

et al. 1996) identified the nucleus of the galaxy with the most obscured and reddened feature of the emission, several arc-seconds SW of the brightest optical emission near the center of the dust lane and consistent with the IR results.

While the discovery of gas disks at the centers of nearby galaxies with *HST* has opened up new possibilities for determining masses of central black holes by studying kinematics of the disks (see Harms et al. 1994; Ferrarese, Ford, & Jaffe 1996; Macchetto et al. 1997; Bower et al. 1998), the dust lane does not permit such studies for NGC 5128 in the optical. We report here *HST* NICMOS observations at 2.2 μm and Pa α which allow us, for the first time, to study the structure of the circumnuclear region at high resolution. We summarize the observations and data reduction in § 2 and the results in § 3. We discuss the implications of these data for standard AGN and jet models in §§ 4 and 5. Throughout we assume a distance to Centaurus A of 3.5 Mpc (Hui et al. 1993), whence $1'' \approx 17$ pc.

2. OBSERVATIONS AND DATA REDUCTION

The nuclear region of NGC 5128 was observed for three orbits on 1997 August 11 using NICMOS camera 2 ($0''.075$ pixel⁻¹) with F222M, F187N, and F190N filters. All observations were carried out with a MULTIACCUM sequence (MacKenty et al. 1997), and the detector was read out non-destructively several times during each integration to facilitate removal of cosmic rays and saturated pixels. The integration times were 2304 s for the F187N and F190N filters (Pa α and adjacent continuum) and 1280 s for the F222M filter (2.2 μm medium-band continuum). The last observation was also performed off-source to enable telescope thermal background subtraction. The data were calibrated using the pipeline software

¹ Based on observations with the NASA/ESA *Hubble Space Telescope*, obtained at the Space Telescope Science Institute, which is operated by AURA, Inc., under NASA contract NAS 5-26555 and by STScI grant GO-3594.01-91A.

² Current address: Osservatorio Astrofisico di Arcetri, Largo E. Fermi 5, 50125 Firenze, Italy.

³ Dipartimento di Astronomia e Scienza dello Spazio, Università di Firenze, Largo E. Fermi 5, 50125 Firenze, Italy.

⁴ Associated with Astrophysics Division, Space Science Department, ESA.

⁵ On leave from Nuffield Radio Astronomy Laboratory, Jodrell Bank, University of Manchester, England, UK.

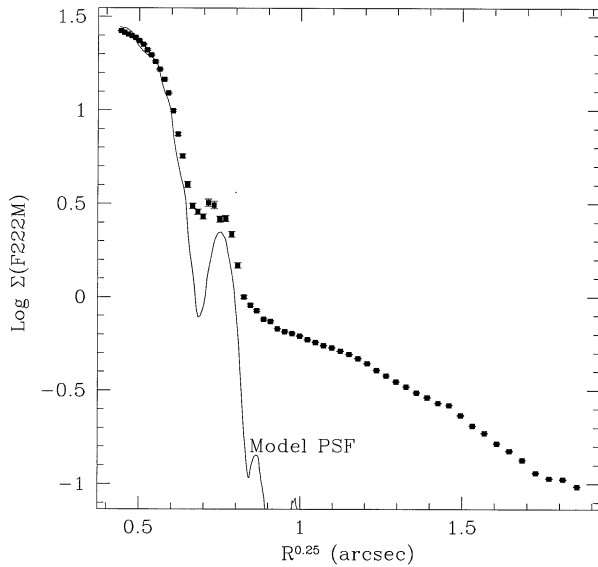


FIG. 2.—Radial light distribution in F222M (filled squares). The logarithm of the azimuthally averaged surface brightness derived from ellipse fitting (units of 10^{-15} ergs cm^{-2} s^{-1} \AA^{-1} arcsec^{-2}) is plotted as a function of the quartic root of the distance from the nucleus. Error bars are comparable to or smaller than the squares. Solid line: the best-fitting model PSF.

CALNICA v3.0 (Bushouse et al. 1997) and the best reference files in the Hubble Data Archive to produce flux calibrated images.

A continuum-subtracted Pa α image was obtained by direct subtraction of the F187N and F190N images. We verified the continuum subtraction by rescaling the continuum by up to $\pm 10\%$ before subtraction and establishing that this did not significantly affect the observed emission-line structure.

A small (few percent) drift in the NICMOS bias level resulted in spatially dependent residuals in the calibrated images (the “pedestal” problem; Skinner, Bergeron, & Daou 1997). This effect was removed by fitting and subtracting a first-degree polynomial surface to each quadrant of the continuum-subtracted images.

3. RESULTS

The calibrated $2.2 \mu\text{m}$ continuum image in Figure 1 (Plate L6) shows the rather smooth and regular structure expected for a typical elliptical galaxy. This smooth structure on small scales contrasts strongly with the patchy and irregular emission observed on the same spatial scales in R and I with WFPC 1 (Schreier et al. 1996). The continuum image is dominated by a strong unresolved source that we interpret as the nucleus of the galaxy.

The intensity of the nucleus is estimated by fitting a model point-spread function (PSF) derived using the TinyTim software (Krist & Hook 1997). We took particular care in removing the PSF artifacts present beyond the first Airy ring. The total nonstellar plus stellar flux of the unresolved nuclear source is $(2.3 \pm 0.1) \times 10^{-15}$ ergs cm^{-2} s^{-1} \AA^{-1} (magnitude 10.52 ± 0.05 in the Vega reference system). Figure 2 shows the azimuthally averaged radial light profile obtained by fitting ellipses to the isophotes in the F222M image and comparing with the model PSF fitted to the data.

The nucleus position is R.A. = 13:25:27.46, decl. = $-43:01:10.2$ (J2000), with the $\pm 1''$ uncertainty of the *HST* Guide Star Catalog (GSC). This position is consistent with that found

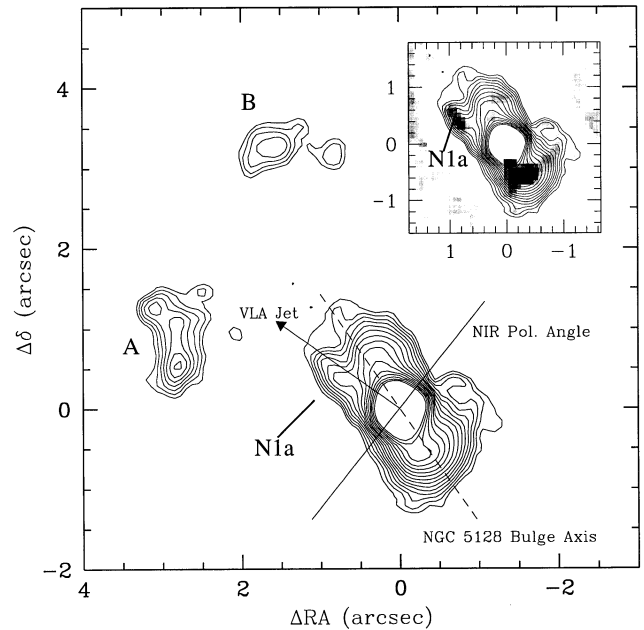


FIG. 4.—Isophotes of the Pa α emission near the nucleus. Contours have constant logarithmic spacing from 6.2 to 53 (units of 10^{-15} ergs cm^{-2} s^{-1} arcsec^{-2}). The origin is the nucleus position. Arrow, the P.A. of the VLA radio jet (Clarke et al. 1986); solid line, the K -band polarization vector ($2''25$ aperture on the IR peak; Packham et al. 1996); dashed line, the position angle from V -band isophotal ellipse fitting of the large-scale NGC 5128 bulge (Dufour et al. 1979). Gray scales in the inset are residuals obtained by subtracting the fitted elliptical model; dynamic range is 2.2–11 (same units).

in the radio and ground-based IR data, and with both the peak of reddening and the peak of polarization found with WFPC 1.

In contrast to the relatively smooth light distribution seen in F222M, the continuum-subtracted Pa α image (Fig. 3 [Pl. L7]) reveals a number of emission features above the threshold of 6×10^{-15} ergs cm^{-2} s^{-1} arcsec^{-2} (3σ of the noise measured in emission-free areas). In addition to the unresolved nuclear source, there is a prominent elongated structure, with some substructure, centered on the nucleus, a finger (N1a) $\approx 0''.9$ NE of the nucleus, two arclike filaments (A, B) located, respectively, at $\approx 2''.9$ NE and $3''.5$ NNE of the nucleus, and several other weaker emission knots and filaments distributed over the field of view.

The dominant feature by far is the structure around the nucleus. Isophotal ellipse fitting gives an average ellipticity of 0.5 and a constant position angle of 33° outside a radius of $\sim 0''.1$, within which the nucleus dominates. The total extension along the major axis is $\approx 2''.3$ (≈ 40 pc), and the total flux from the extended nuclear emission above the level of 1.1×10^{-14} ergs cm^{-2} s^{-1} arcsec^{-2} is $(3.9 \pm 0.4) \times 10^{-14}$ ergs cm^{-2} s^{-1} . In comparison, the observed flux from the unresolved Pa α emission is $(5.7 \pm 0.6) \times 10^{-14}$ ergs cm^{-2} s^{-1} . The inset in Figure 4 overlaying the Pa α contours on a gray-scale plot of the nuclear emission after subtracting the isophotal fit model clearly shows N1a and another substructure SSE of the nucleus.

4. EXTENDED Pa α DISK

The elongated structure around the nucleus seen in Pa α emission has an overall extent of $\sim 40 \times 20$ pc. Its position angle of 33° is approximately perpendicular to that of the dust lane. It is not oriented along the axis of the X-ray/radio jet, which

has a position angle of $\sim 50^\circ$ – 55° as seen at X-ray (Schreier et al. 1979), centimeter (Burns et al. 1983), and VLBI (Jones et al. 1996) wavelengths. It is also not perpendicular to the jet axis, as reported for an extended structure seen with ISOCAM at much lower resolution in the near IR at P.A. $\sim 145^\circ$ (Vigroux 1998), nor is it consistent with the orientation of a ring with a radius of ≈ 100 pc perpendicular to the radio jet, reported by Rydbeck et al. (1993). As such, we believe that we are observing a new feature, not directly related to the radio/X-ray jet or to any previously reported optical or IR features.

We have verified that the observed elongation is not the result of varying extinction in front of a smooth circular emission region. Indeed, if the extinction is maximum at the nucleus and decreases outward in a direction perpendicular to the dust lane, the resulting morphology would be elongated in the direction of this extinction gradient. We calculated the IR reddening correction map by adopting the procedure presented in Schreier et al. (1996), comparing the colors obtained in recent WFPC 2 observations (Schreier et al. 1998) with our NICMOS continuum images, using the reddening law of Cardelli, Clayton, & Mathis (1989) with $R_V = 3.1$ and assuming a constant intrinsic color over the field of view of NICMOS; this latter assumption is supported by an $I - K$ versus $V - I$ color diagram, where most of the points lie tightly along the reddening line. Applying the derived reddening correction to the Pa α image does not significantly affect the morphology of the observed structure.

HST observations of other AGNs suggest three possible explanations for the observed elongated structure: (1) gas that is shocked and compressed by interaction with the jet; (2) illumination of gas clouds by an anisotropic nuclear radiation field (i.e., an ionization cone; see Robinson 1997 and references therein); and (3) a gaseous disk, such as that of M87 (Harms et al. 1994).

The structure's position angle differs by $\sim 20^\circ$ from the jet axis (see Fig. 4). This significant misalignment suggests the emission is not caused by a current jet-cloud interaction, especially when we see other Pa α features well correlated with the radio/X-ray jet morphology (see 5). It has long been hypothesized that the radio jet had a different (smaller) position angle in the past, creating the N–S orientation of the outer lobes and then rotating to form first the inner lobes and then the currently observed X-ray/radio jet. In this regard we note that the outer edge of the NE inner lobe does have structure aligned with the position angle of our feature; both could be gas shocked by the jet (perhaps two-sided) at some recent time, and not yet cooled down. Existing radio and X-ray measurements do not provide added information on this small spatial scale.

The $\sim 20^\circ$ misalignment with the jet does allow the elongated structure to lie well within a putative ionization cone. We note that most of the other detected emission features would also lie within such a cone if it has an opening half-angle of at least $\sim 30^\circ$, well within the limits postulated by the unified model (see, e.g., Antonucci 1993). As it stands, we cannot rule out clouds densely distributed along this position angle, embedded in a large opening angle radiation field. However, the relative thickness of the feature in the transverse direction and the symmetry around the nucleus suggest that this is not the case.

We find the simplest interpretation for the elongated emission to be a gaseous disk around the nucleus, as seen on larger scales around other galactic nuclei. It could be the outer part of an accretion disk, expected around a massive black hole at the core of this AGN. If the structure is indeed a thin circular

disk, the axial ratio suggests an inclination of $\approx 60^\circ$. Its radius of $\sim 1/2$ (~ 20 pc) makes it significantly smaller than the 100 pc scale stellar disks observed by *HST* at the centers of many galaxies.

This gas disk could be readily ionized by the powerful AGN, seen in X-rays and γ rays. The flux of photons required to keep the Pa α emitting material ionized can be computed following Osterbrock (1989): after dereddening ($A_V = 10$ mag) and assuming Case B recombination for $T_e = 10^4$ K and $N_e = 10^3$ cm $^{-3}$, we find a value of 4×10^{51} photons s $^{-1}$. This is a small fraction of the total expected emission from the AGN. Note that the nucleus has an extinction of up to 70 mag along the line of sight, estimated from X-ray observations. However, while being within the ionization cone the disk is well outside the obscuring torus and subject to a much lower extinction from the nucleus. We thus assume $A_V = 10$ mag as a reasonable upper estimate of the foreground extinction, following Schreier et al. (1996), who found a peak extinction of $A_V = 7$ mag in the optical.

The mass of the gas responsible for both extended and unresolved nuclear emission is estimated from the standard relation, $L(\text{Pa}\alpha) = N_p N_e V 4\pi J(\text{Pa}\alpha) = N_e 4\pi J(\text{Pa}\alpha) M/m_H$:

$$M = 1.2 \times 10^4 M_\odot F_{-13}^{\text{obs}}(\text{Pa}\alpha) 10^{0.059(A_V-10)} \left(\frac{N_e}{10^3}\right)^{-1}, \quad (1)$$

where N_p is the proton density, V is the volume of the emitting gas, $J(\text{Pa}\alpha)$ is the line emissivity, m_H is the proton mass, $F_{-13}^{\text{obs}}(\text{Pa}\alpha)$ is the observed Pa α flux in units of 10^{-13} ergs cm $^{-2}$ s $^{-1}$, and $10^{0.059(A_V-10)}$ is the reddening correction if A_V is different from the assumed 10 mag. This modest mass estimate of $M \sim 10^4 M_\odot$ depends mostly on the assumed gas density ($N_e = 10^3$ cm $^{-3}$) and is extremely uncertain, but we believe that a disk of 10^3 – $10^5 M_\odot$ is quite feasible.

The Pa α disk is consistent with being perpendicular to the plane of the dust lane and lying along the major axis of the large elliptical galaxy (see Fig. 4). It is now widely accepted that the large gas/dust disk of Cen A (i.e., the dust lane) was acquired in a recent merger process and that differential precession has led to the observed warped structure (see, e.g., Tubbs 1980). In the central region of Cen A, the precession time is only 10^7 yr, and the orthogonal alignment of our small disk may be consistent with numerical studies of the evolution of gas disks in bulge systems (see, e.g., Quillen et al. 1992). If we thus interpret the observed emission as being from the warped outer portions of an accretion disk around the active nucleus, we conclude that even on the relatively small spatial scale of a few parsecs, the disk is dominated by the gravitational potential of the galaxy as a whole and not by the symmetry of the AGN and its jet.

For a nonrotating black hole (BH), one would expect the jet to have its direction determined by the angular momentum axis of the inner gaseous disk, while for a Kerr black hole, it would be expected to be aligned along the spin axis of the black hole itself (Bardeen & Petterson 1975). Close to a Kerr BH, ($r \approx Gm/c^2 \sim 10^{14}$ cm $\sim 10^{-4}$ pc), the disk itself will warp to become normal to the spin axis. In our Cen A data, on a few parsec scale, the normal to the Pa α disk and the radio jet are misaligned by $\sim 70^\circ$ in projection. We conclude that if Cen A contains a rotating black hole, then either the gas disk must be outside the sphere of influence of the black hole or it was formed recently enough that it has not yet become aligned with the spin axis; for a nonrotating black hole, we find that the

disk must become significantly warped away from being normal to the jet inside a radius of ~ 2 pc.

Pringle (1997) has recently modeled self-induced warping of accretion disks in AGNs. He finds that disks are likely to be warped at $R > 0.02$ pc around a $\sim 10^8 M_{\odot}$ BH. Our results show a constant position angle for the disk in to ~ 2 pc, suggesting the somewhat weak upper limit of $\sim 10^{10} M_{\odot}$ for the mass of the black hole.

5. Pa α FEATURES RELATED TO THE X-RAY/RADIO JET

Three of the relatively strong Pa α features detected appear spatially associated with the X-ray/radio jet of Centaurus A. In Figure 5 (Plate L8) we overlay the Pa α image with a 6 cm radio map (E. Feigelson 1997, private communication; see also Fig. 1 of Clarke et al. 1986). We align the two images assuming that the radio and NIR nuclei are coincident and note that the extended N-S extent of the radio contours is the result of the 0.3×1.1 radio beam.

The kiloparsec-scale X-ray/radio jet has an average P.A. = $55^{\circ} \pm 7^{\circ}$, the innermost knots have a slightly larger P.A. $\approx 60^{\circ}$, and the VLBI milliarcsecond jet and counterjet (see Jones et al. 1996) are at P.A. $\approx 51^{\circ} \pm 3^{\circ}$. We note that the multiple components of the radio jet within a few arcseconds of the nucleus were not resolved by Burns et al. (1983) and were reported as N1. They are clearly visible in the contour map (Fig. 5) and Figure 1 of Clarke et al. (1986), as part of their $6''$ nuclear jet, although the individual components were not discussed. We label the compact, innermost knot N1a and see that it corresponds positionally with the Pa α "finger" $\approx 0.9''$ from the nucleus at P.A. $\approx 64^{\circ} \pm 11^{\circ}$ (see also Fig. 4, *inset*). The two Pa α arcs A and B, at distances of $\approx 2.9''$ and $\approx 3.5''$ from the nucleus, each extending over ≈ 20 pc, are seen to lie ≈ 15 and 30 pc, respectively, on either side of another knot of the nuclear jet. These may result from an outgoing shock created by interaction between the radio-emitting nuclear ejecta and a gas cloud. We note that the radio jet has a steep spectrum at this distance from the nucleus (Clarke et al. 1986), suggesting that the gas is still too hot along the jet axis to show line emission. We can expect, with adequate resolution, to see X-ray emission from this region of the jet.

6. SUMMARY

We summarize the key results of our $2.2 \mu\text{m}$ continuum and Pa α observations of the inner region of NGC 5128 as follows:

1. We see an extended continuum source with the rather regular and smooth structure expected for an elliptical galaxy. This smoothness contrasts strongly with the filamentary structure observed in the WFPC *I*-band image.

2. We identify a strong unresolved ($r < 0.1''$) central source as the nucleus of the galaxy. Its position is consistent with ground-based IR and radio data and the peak of reddening and polarization found with WFPC 1. The nucleus has an intensity of $(2.3 \pm 0.1) \times 10^{-15}$ ergs $\text{cm}^{-2} \text{s}^{-1} \text{\AA}^{-1}$ based on our continuum observations and a flux of $(5.7 \pm 0.6) \times 10^{-14}$ ergs $\text{cm}^{-2} \text{s}^{-1}$ in Pa α .

3. We see a prominent elongated structure in Pa α centered on the nucleus, with a major to minor axis ratio of ~ 2 , extending $\approx 2''$ along position angle $\approx 33^{\circ}$ perpendicular to the dust lane. We interpret this as an inclined ~ 40 pc diameter thin nuclear disk of ionized gas.

4. We see several smaller Pa α features, including three relatively strong ones, which appear spatially related to the X-ray/radio jet. We interpret them as circumnuclear gas clouds shocked by the jet.

The disk, with a radius of $\sim 1.2''$, corresponding to ~ 20 pc at 3.5 Mpc, is among the smallest ever observed at the nucleus of an AGN in the optical/near-IR. It is significantly smaller than the 100 or more parsec stellar disks presumed to exist at the centers of many galaxies. Even at this small scale, the disk is not perpendicular to the jet. It is, however, consistent with being perpendicular to the dust lane and oriented along the major axis of the bulge. If it represents the warped outer portion of an accretion disk around the active nucleus, we conclude that even a few parsecs from the nucleus, the disk is dominated by the galaxy gravitational potential and not by the symmetry of the AGN and its jet.

Further NICMOS observations are planned in $2 \mu\text{m}$ polarized light and [Fe II] to provide emission mechanism diagnostics and determine the geometry of the nuclear radiation field. If a warped disk illuminated by the nucleus is the correct model, systematic changes in the polarization angle as a function of disk position should be seen. High spatial resolution infrared spectroscopy is planned to measure gas kinematics in the disk and thus determine the mass of the black hole.

A. M. and N. C. acknowledge support through GO grants G005.44800, G005.76700, and G005.70200 from Space Telescope Science Institute, which is operated by the Association of Universities for Research in Astronomy, Inc., under NASA contract NAS 5-26555. We thank Howard Bushouse, Alex Storrs, John Mackenty, Chris Skinner, Eddy Bergeron, and other STScI NICMOS staff for invaluable assistance in understanding the NICMOS instrument and its calibration. We thank Nino Panagia, Martino Romaniello, Ernesto Oliva, George Miley, and Gary Bower for useful comments and discussions. We thank Eric Feigelson for providing an unpublished radio map and Zolt Levay for help in producing plates for this Letter.

REFERENCES

- Antonucci, R. R. J. 1993, *ARA&A*, 31, 473
 Bailey, J., Sparks, W. B., Hough, J. H., & Axon, D. J. 1986, *Nature*, 322, 150
 Bardeen, J. M. & Petterson, J. A. 1975, *ApJ*, 195, 65
 Blandford, R. D. 1991, in *Proc. Heidelberg Conf., Physics of AGN*, ed. W. J. Duschl & S. J. Wagner (Berlin: Springer), 3
 Bower, G. A., et al. 1998, *ApJ*, in press
 Burns, J. O., Feigelson, E. D., & Schreier, E. J. 1983, *ApJ*, 273, 128
 Bushouse, H., Skinner, C. J., & MacKenty, J. W. 1997, *NICMOS Instrument Sci. Rept. 97-28* (Baltimore: STScI)
 Cardelli, J. A., Clayton, G. C., & Mathis, J. S. 1989, *ApJ*, 345, 245
 Clarke, D. A., Burns, J. O., & Feigelson, E. D. 1986, *ApJ*, 300, L41
 Dufour, R. J., et al. 1979, *AJ*, 84, 284
 Feigelson, E. D., Schreier, E. J., Delvaile, J. P., Giacconi, R., Grindlay, J. E., & Lightman, A. P. 1981, *ApJ*, 251, 31
 Ferrarese, L., Ford, H. C., & Jaffe, W. 1996, *AJ*, 470, 444
 Harms, R. J., et al. 1994, *ApJ*, 435, L35
 Hui, X., Ford, H. C., Ciardullo, R., & Jacoby, G. H. 1993, *ApJ*, 414, 463
 Krist, J. E., & Hook, R. 1997, *TinyTim User Guide, Version 4.4* (Baltimore: STScI)
 Jones, D. L., et al. 1996, *ApJ*, 466, L63
 MacKenty, J. W., et al. 1997, *NICMOS Instrument Handbook, Version 2.0* (Baltimore: STScI)
 Macchetto, F. D., Marconi, A., Axon, D. J., Capetti, A., Sparks, W. B., & Crane, P. 1997, *ApJ*, 489, 579

- Osterbrock, D. E. 1989, *Astrophysics of Gaseous Nebulae and Active Galactic Nuclei* (Mill Valley: University Science Books), 146
- Packham, C., Hough, J. H., Young, S., Chrysostomou, A., Bailey, J. A., Axon, D. J., & Ward, M. J. 1996, *MNRAS*, 278, 406
- Pringle, J. E. 1997, *MNRAS*, 292, 136
- Quillen, A. C., de Zeeuw, P. T., Phinney, E. S., & Phillips, T. G. 1992, *ApJ*, 391, 121
- Robinson, A. 1997, in *ASP Conf. Ser. 113, Emission Lines in Active Galaxies: New Methods and Techniques*, ed. B. M. Peterson, F.-Z. Cheng, & A. S. Wilson (San Francisco: ASP), 280
- Rydbeck, G., Wiklind, T., Cameron, M., Wild, W., Eckart, A., Genzel, R., & Rothermel, H. 1993, *A&A*, 270, L13
- Schreier, E., Burns, J. O., & Feigelson, E. D. 1981, *ApJ*, 251, 523
- Schreier, E. J., Capetti, A., Macchetto, F., Sparks, W. B., & Ford, H. C. 1996, *ApJ*, 459, 535
- Schreier, E. J., Feigelson, E., Delvaile, J., Giacconi, R., Grindlay, J., Schwartz, D. A., & Fabian, A. C. 1979, *ApJ*, 234, L39
- Schreier, E. J., Marconi, A., Capetti, A., Caon, N., Axon, D., Macchetto, F. 1998, in preparation
- Skinner, C. J., Bergeron, L. E., & Daou, D. 1998, *HST Calibration Workshop*, ed. S. Casertano et al. (Baltimore: STScI), in press
- Tubbs, A. D. 1980, *ApJ*, 241, 969
- Vigroux, L. 1998, *IAU Symp. 186, Galaxy Interactions at High and Low Redshift* (Dordrecht: Kluwer), in press

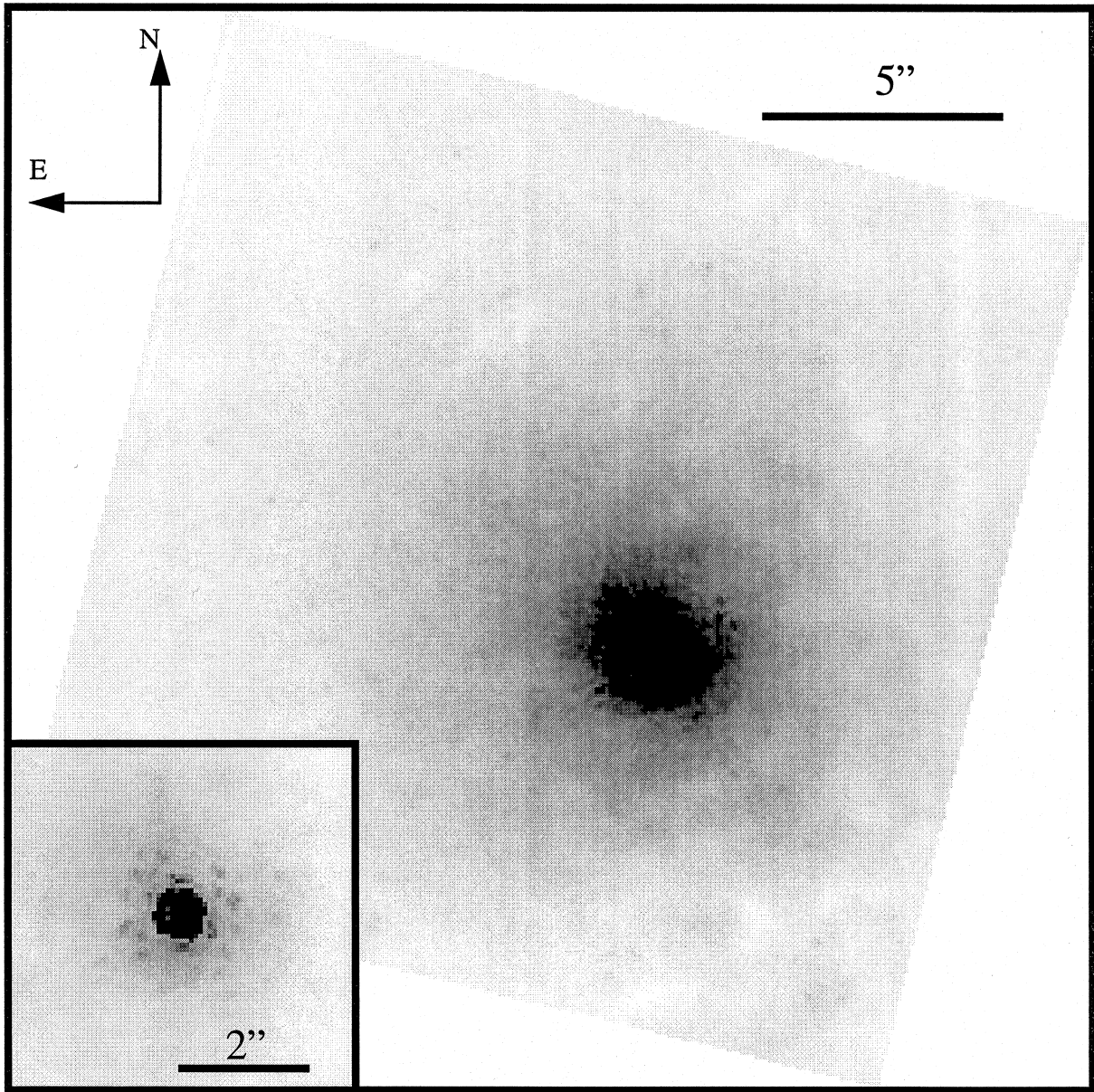


FIG. 1.—Gray-scale F222M image of the nuclear region; dynamic range is 0.45–6.2 (units of 10^{-16} ergs cm^{-2} s^{-1} \AA^{-1} arcsec^{-2}). Inset shows the region around the unresolved source identified as the nucleus; dynamic range is 3.6–14 (same units). Dots and other linear structures are artifacts of the NICMOS PSF.

SCHREIER et al. (see 499, L144)

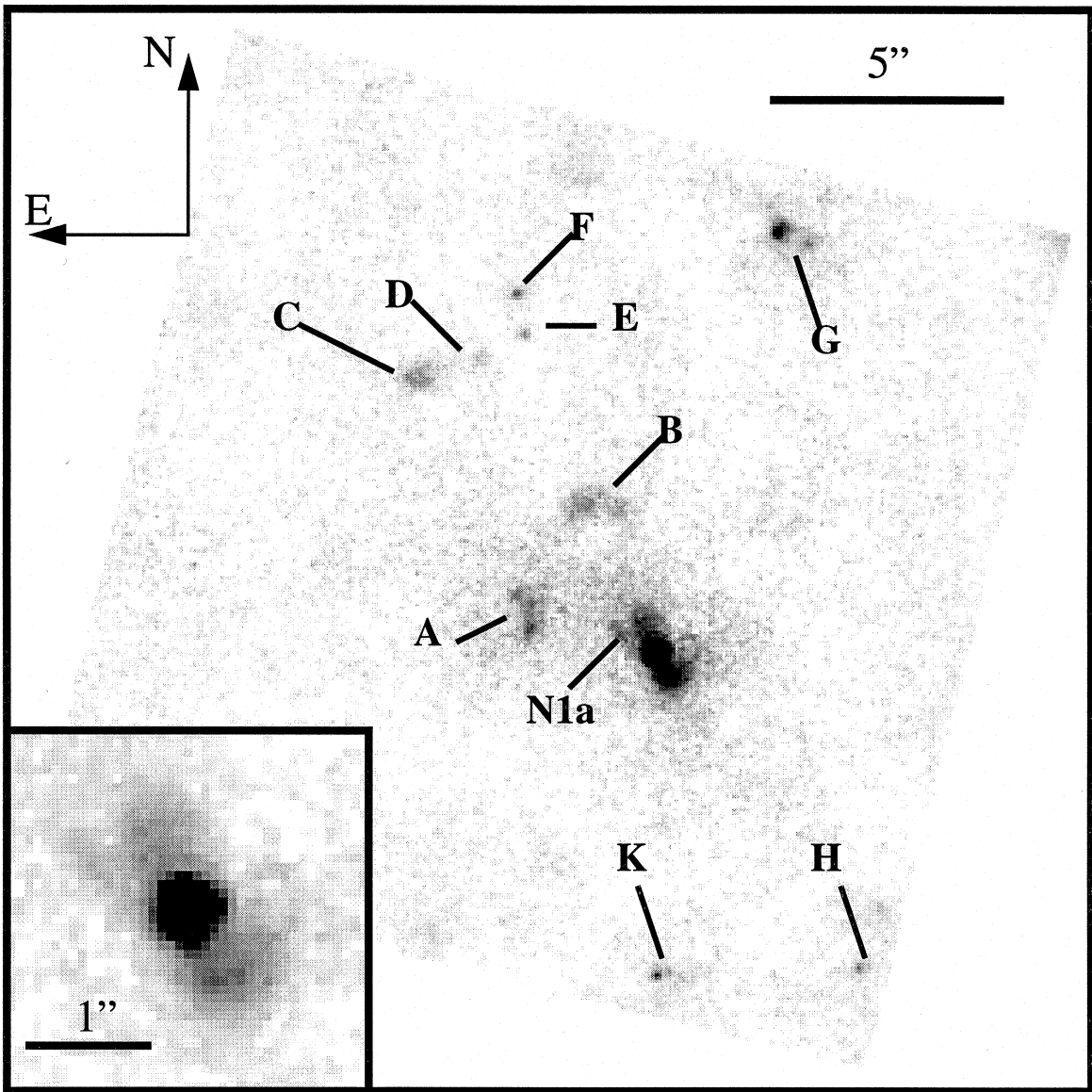


FIG. 3.—Gray-scale continuum-subtracted Pa α image; dynamic range is 0–3.6 (units of 10^{-14} ergs cm^{-2} s^{-1} arcsec^{-2}). Inset shows the central region; dynamic range is 0.18–11 (same units). The emission-line knots and filaments are labeled for reference.

SCHREIER et al. (see 499, L144)

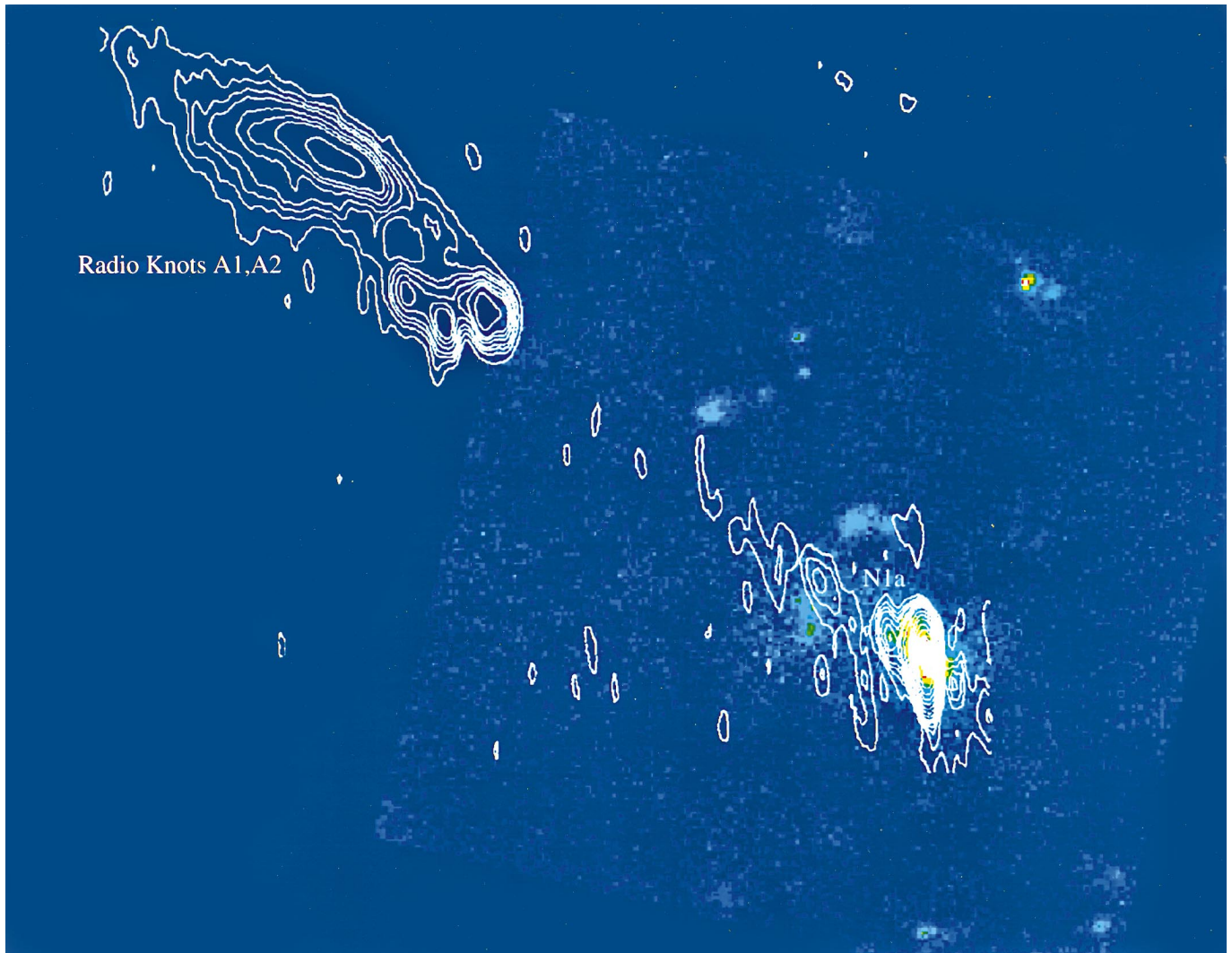


FIG. 5.—6 cm isophotes of the nuclear region of NGC 5128 (E. Feigelson 1997, private communication; see also Clarke et al. 1986) overlaid on our Pac image.

SCHREIER et al. (see 499, L144)